Available online at www.sciencedirect.com
ScienceDirect
Journal of the European Ceramic Society 29 (2009) 1825–1829
www.elsevier.com/locate/jeurceramsoc

Fracture toughness of concentric Si_3N_4-based laminated structures

Zoran Krstic *, Vladimir D. Krstic

Centre for Manufacturing of Advanced Ceramics and Nanomaterials, Queen's University, Nicol Hall, Kingston, Ontario, Canada K7L 3N6

Received 1 May 2008; received in revised form 10 October 2008; accepted 16 October 2008
Available online 25 November 2008

Abstract

A new concentric rectangular laminated structure was designed and fabricated by slip-casting method and densified by pressureless sintering process. One class of laminates consists of layers of Si_3N_4 with 7 wt.% Y_2O_3 and 3 wt.% Al_2O_3 as sintering aids, and of interlayers consisting of 50 wt.% BN and 50 wt.% Al_2O_3 designated as SN-(BN + Al_2O_3). The other class of laminates has the same Si_3N_4 layer composition but different interlayer composition of 90 wt.% BN and 10 wt.% Si_3N_4 designated as SN-(BN + SN). The objective of this paper is to investigate the effects of the number of layers and their thickness on apparent fracture toughness of these laminates. The interfacial layer composition was discussed in terms of its role in toughening of the laminates. For the SN-(BN + Al_2O_3) laminates the highest apparent fracture toughness of 22 MPa $m^{1/2}$ was found in the samples with 7 Si_3N_4 layers and for the SN-(BN + SN) laminates the highest apparent fracture toughness of 19.5 MPa $m^{1/2}$ was found in the samples with 4 Si_3N_4 layers.

Keywords: Silicon nitride; Slip-casting; Fracture toughness; Laminated structures

1. Introduction

Over the last decade there has been concentrated effort to produce structures with crack resistance capabilities approaching those of fiber composites. As a result of this effort, various planar laminated structures were designed and fabricated possessing an apparent fracture toughness and work of fracture significantly higher that those of monolithic counterpart.[1–4] Although the improvements in fracture resistance in these planar laminates were sufficient to ensure their safe use in many structural applications, delamination and easy crack propagation along the weak interface between the two layers has been the major impediment for wider use of these structures (Fig. 1). To overcome this unwanted delamination/peeling problem associated with the plate-form laminates (see Fig. 1) a concentric rectangular design has been developed and fabricated in which the potential delamination direction is completely eliminated.[5,6] In addition of eliminating the direction of easy crack propagation, this new structure exhibits fracture resistance characteristics far beyond those of monolithic ceramics or planar laminates.[7]

The basic concept in this new design is that, as the crack propagates through the base material, it deflects at the weak interfaces oriented transversely to the direction of crack propagation. The path of crack propagation in the circular and rectangular cylinder structures is shown schematically in Fig. 2.

The toughening in these ceramic/ceramic laminates is the crack deflection at the weak interface such that no catastrophic failure occurs. This condition is achieved when the strength of the interface is sufficiently weak to allow the deflected crack to propagate a long distance before changing its direction.

It has been shown by Zhang and Krstic[8] that both the numbers of layers and their thickness play an important role in toughening and strengthening of the planar laminates. In an attempt to model the fracture behaviour of the planar laminates, Clegg[9] assumed that the fracture toughness of the planar laminates is related to the strength of the laminate and the beam thickness (d) as expressed by the equation[9]:

$$K_{IC} = \sigma_f Y \sqrt{c} \left(\frac{1-c}{d} \right)^2 \quad (1)$$

where K_{IC} is the fracture toughness of the laminate, σ_f is the fracture strength, c is the notch length and Y is a constant. Clearly, the toughening in Eq. (1) is based on the level of strength of the laminate which is a reasonable assumption considering that the

* Corresponding author.
E-mail address: krsticz@queensu.ca (Z. Krstic).

0955-2219/$ – see front matter © 2008 Elsevier Ltd. All rights reserved.
doi:10.1016/j.jeurceramsoc.2008.10.007

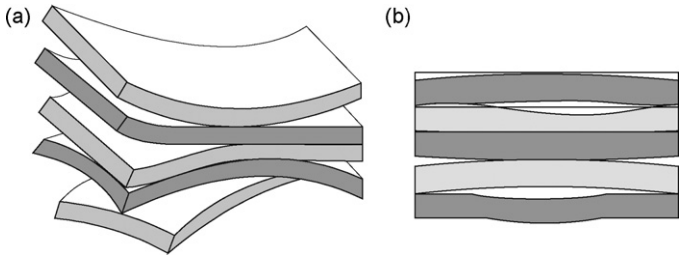

Fig. 1. (a) Peeling and (b) delamination in the plate-form laminates.

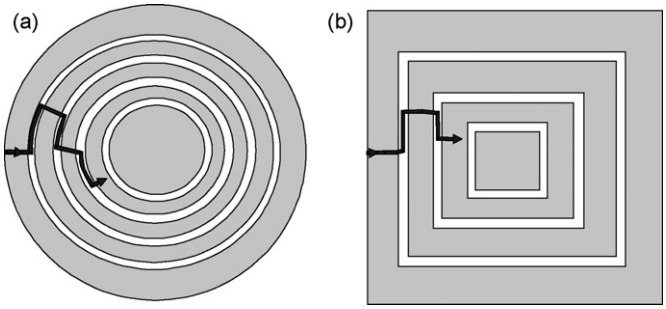

Fig. 2. Schematics of crack deflection in (a) circular and (b) rectangular cross-sectioned concentric laminate structures.

primary crack is blunted and reinitiated at the next layer. This makes the laminate's apparent fracture toughness insensitive to the crack radius.

Shanches-Herencia et al.[3] have showed that the crack extension within the layer occurs only when the layer thickness exceeds a critical value which is directly related to the critical strain energy release rate or fracture toughness:

$$t_c = \frac{G_c E}{0.34}(1-\nu^2)\sigma_r^2 \tag{2}$$

where t_c is the critical layer thickness, E is the Young's modulus, ν is the Poison's ratio, G_c is the critical strain energy release rate and σ_r is the residual stress at the surface of the layer.

Also, Philips et al.[10] showed that the crack deflection in the plate-form laminates does not occur when the ratio between the interfacial critical strain energy release rate G_{IC} and the bulk critical strain energy release rate G_{BC} exceeds unity. According to Philips et al.[10], this condition is achieved when the interfacial toughness is high enough and the performance of the laminate would revert to that of the monolithic materials. The relationship between the interfacial fracture toughness (G_{IC}), the numbers of layers (T) and the layer thickness (δ) is given by the equation:

$$G_{IC} = \sigma_c \frac{\delta}{18E}\left[T - \left(\frac{(T-1)^3}{T^2}\right)\right]$$

where σ_c is the critical stress for failure of the next layer and E is the Young's modulus.

2. Experimental procedure

Concentric Si_3N_4/BN laminates are fabricated by slip-casting alternate layers of Si_3N_4 and BN employing the previously developed modified slip-casting method.[8] High purity α-Si_3N_4 powder was used as a raw material. Sub-micron size Al_2O_3 (A-16, Alcoa) and Y_2O_3 (Alpha Aesar) powders were used as sintering aids. BN powder (Carborundum Co., grade HPP-325) with the addition of Al_2O_3 and Si_3N_4 was used for casting weak interlayers. After drying, pressureless sintering was done in a graphite resistance furnace (Vacuum Industries, USA) at temperatures ranging from 1740 °C to 1800 °C for 1 h under static N_2 gas atmosphere.

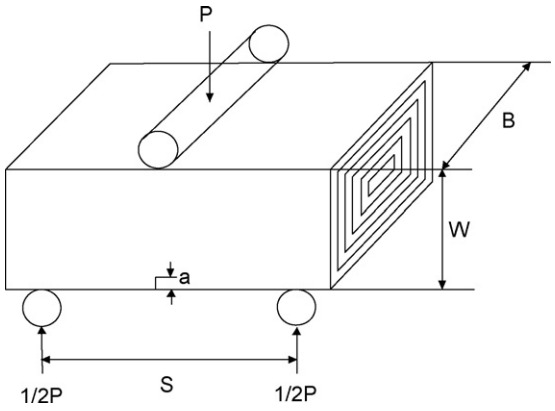

Fig. 3. Sample configuration for three-point bending test with corresponding dimensions.

Fracture toughness was measured using the three-point bending test at room temperature with a straight-through notch introduced in the mid-section of the samples (Fig. 3). The notch was introduced by a 500 μm thick diamond wheel through the first or first two layers and its depth (~750–1220 μm) was measured under an optical microscope with 50× or 100× magnifications. The initial crack radius does not play significant role since the crack has to be reinitiated on the next layer creating an inherently sharp crack. The test was carried out on an Instron machine (Model 8502 FIB, Instron Co., Canton, USA) using a jig with the span of 26 mm and the crosshead speed of 0.06 mm/min. Five samples were tested per data point. The fracture toughness was calculated using the equation[11]:

$$K_{IC} = \frac{P}{BW^{1/2}} \cdot \frac{S}{W} \cdot \frac{3\alpha^{1/2}}{2(1-\alpha)^{3/2}} \cdot Y \tag{4}$$

where K_{IC} is the fracture toughness, P is the maximum load at fracture, S is the span, B is the sample width, W is the sample height, α is the coefficient ($\alpha = a/W$; a the notch depth) and Y is the stress intensity factor coefficient, which is expressed by the equation:

$$Y = 1.9887 - 1.326\alpha - (3.49 - 0.68a + 1.35\alpha^2)\alpha(1 - \alpha)(1 + \alpha)^{-2} \tag{5}$$

3. Results and discussion

There are several important mechanical parameters which determine the engineering application of any material. In the present work, the emphasis was placed on the fracture toughness. Fig. 4 shows the change of the apparent fracture toughness

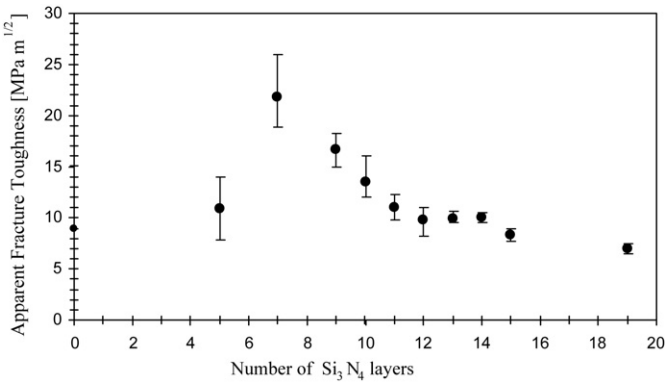

Fig. 4. Variation of apparent fracture toughness of SN-(BN + Al_2O_3) with the number of Si_3N_4 layers.

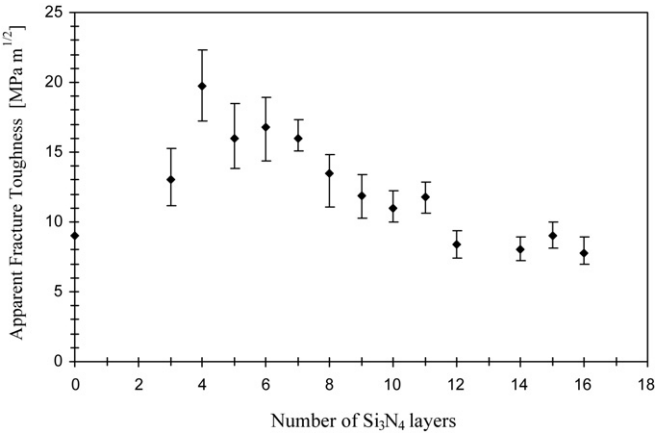

Fig. 5. The effect of the number of Si_3N_4 layers on apparent fracture toughness of SN-(BN + SN).

with the number of Si_3N_4 layers for SN-(BN + Al_2O_3) laminates. Here, the term apparent fracture toughness is used instead of fracture toughness to indicate that the fracture toughness measurements were done on the materials where the crack initiation was responsible for fracture rather then the propagation of sharp crack. Even though the sharp crack was not introduced initially, it has been observed that this primary crack is deflected by the weak interface and the new crack is initiated at the next Si_3N_4 layer, making the entire system independent on the sharpest radius of the primary crack. As shown in Fig. 4, the apparent fracture toughness increases with an increase of number of Si_3N_4 layers up to 7 layers and then the fracture toughness decreases. The highest apparent fracture toughness of 22 MPa m$^{1/2}$ was measured in samples having 7 Si_3N_4 layers. The lowest apparent fracture toughness of 8 MPa m$^{1/2}$ was found in samples with 19 Si_3N_4 layers. The initial increase in the apparent fracture toughness in samples with 5–7 layers is due to the fact that a certain minimum number of layers is required to avoid the crack reaching the core of the sample which was made of monolithic Si_3N_4 (non-laminated) which has fracture toughness of only 9 MPa m$^{1/2}$. It appears that, for the samples with the number of layers between 5 and 7, the ability of the interface to deflect the crack is the highest, thus leading to the maximum toughening. Once the crack is deflected, it can propagate only a certain distance along the interface before its stops. Its initiation at the surface of the next Si_3N_4 layer requires higher stress compared to that one for the propagation of the existing crack. Thus, in this region, the fracture toughness increases with the number of layers. As shown in Fig. 4, after a certain number of layers (7 in the present work) the overall toughness decreases to ~8 MPa m$^{1/2}$ which is very close the level of the fracture toughness measured in monolithic Si_3N_4.[12] A possible reason for the decrease in the apparent fracture toughness for the samples having more than 7 Si_3N_4 layers is the decrease in thickness of the Si_3N_4 layers and BN-based interfacial layer as the number of layers is increased. The measurement of the layer thickness revealed that, as the number of the Si_3N_4 layers increases, the layer thickness decreases. When the thickness of the Si_3N_4 layer becomes too small, the laminates tend to exhibit its fracture behaviour closer to that of a monolithic ceramic (K_{IC} ~9 MPa m$^{1/2}$), measured by the three-point bending test, with no ability to deflect the propagating crack. It is also found that, as the number of the layers in the sample exceeds some critical number the ability of the crack to deflect becomes smaller and smaller. This trend was found to exist in both laminates SN-(BN + SN) and SN-(BN + Al_2O_3), as shown in Fig. 5.

Again, as with other laminates, there is an increase in the apparent fracture toughness with the number of Si_3N_4 layers reaching a maximum at a certain number of layers, followed by a decrease of the fracture toughness. In the SN-(BN + SN) laminates, the highest apparent fracture toughness of 19.5 MPa m$^{1/2}$ was measured in the sample having 4 Si_3N_4 layers. When this value for the fracture toughness is compared with those of SN-(BN + Al_2O_3) it is found that the fracture toughness of the SN-(BN + Al_2O_3) laminates is higher than that of the SN-(BN + SN) laminates. This difference in the fracture toughness between the two composites is associated with the ability of the interface to deflect the propagating crack. When it comes to Si_3N_4 layers, the toughness of Si_3N_4 layer must be sufficiently high to prevent an easy crack initiation at the surface of the next layer. An example of the microstructure showing a weak and porous interface and a dense and tough Si_3N_4 layers is shown in Fig. 6. The microstructure shown in Fig. 6 is the one that consists of a weak and/or porous interface and a dense and strong Si_3N_4 layers and exhibits the highest fracture toughness (Fig. 6(b)).

It is also interesting to note from Fig. 6(a) that there are a number of β-Si_3N_4 grains sticking out from the of Si_3N_4 layers indicating that the interface provides the vehicle for growth of the elongated grains from one layer of Si_3N_4 to another crossing the weak interface. It is believed that this interfacial bridging contributes to high apparent fracture toughness in these laminates.

The effect of thickness of the Si_3N_4 layers on the fracture toughness is shown in Figs. 7 and 8. The highest apparent fracture toughness was found for the laminates with the layer thickness between 200 μm and 250 μm. The apparent fracture toughness as high as 22 MPa m$^{1/2}$ was obtained in the laminates having an average layer thickness of ~230 μm. These maximum in the fracture toughness at a particular Si_3N_4 layer thickness, occurs in all samples where the ratio of Si_3N_4 layer thickness to BN interlayer thickness (~12–15 μm) is around 20.

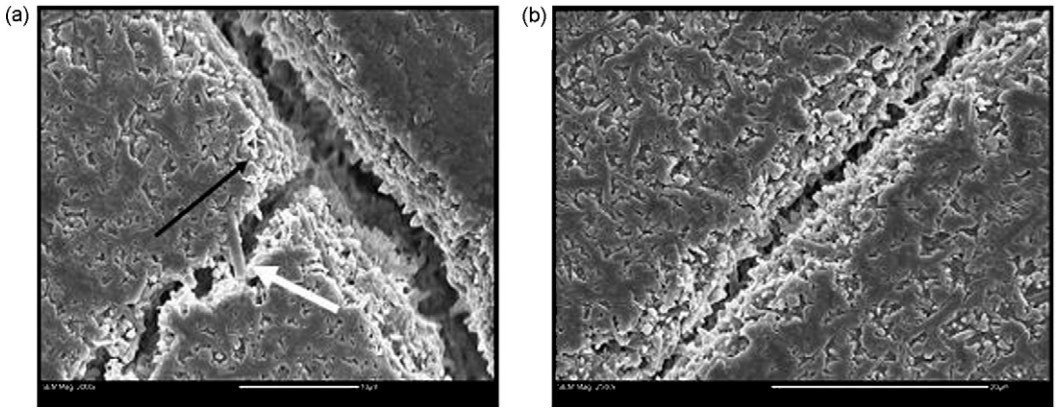

Fig. 6. (a) Micrograph of an etched surface showing the direction of the crack propagation (pointed by the black arrow) and the bridging grain pull out at the surface of the crack at the weak interface (the white arrow). (b) A weak/porous interfaces between dense and strong Si_3N_4 layers.

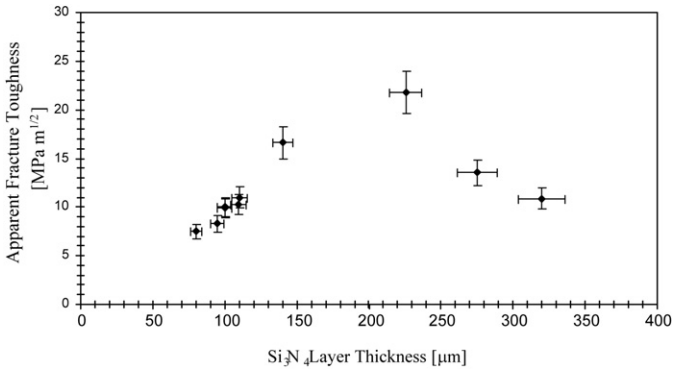

Fig. 7. Effect of Si_3N_4 layers thickness on fracture toughness of SN-(BN + Al_2O_3) laminated structure.

The decrease in the fracture toughness at higher Si_3N_4 layer thickness is considered to be caused by a decrease in the number of interfaces available for crack deflection and responsible for toughening and strengthening.

Fig. 8 depicts the effect of the Si_3N_4 layers thickness on the apparent fracture toughness of the SN-(BN + SN) laminates. Unlike the SN-(BN + Al_2O_3) laminates, which show maximum in the apparent fracture toughness at Si_3N_4 layer thickness of ~230 μm, the SN-(BN + SN) laminates exhibit maximum in the apparent fracture toughness of 19.5 MPa $m^{1/2}$ at thickness of ~450 μm. The evaluation of the relationship between Si_3N_4 and BN layer thickness reveals that there is an optimum thickness ratio for Si_3N_4/BN of ~30 for the SN-(BN + SN) laminates and ~20 for SN-(BN + Al_2O_3) laminates. The lowest apparent fracture toughness of ~8 MPa $m^{1/2}$ is observed with the samples having the ratio of Si_3N_4 layers to BN layers thickness of ~6 which is almost identical to that of SN-(BN + Al_2O_3) laminates.

It is worth noting that difficulties were experienced in keeping the thickness of the Si_3N_4 layers constant as the number of the layers increased. This difficulty stems from the fact that, as the number of the layers increases, so does the wall thickness leading to reduced rate of the particle deposition. In order to eliminate the effect of number of the layers on the fracture toughness, a series of tests were conducted where the number of the Si_3N_4 layers was kept constant. The results are shown in Fig. 9 for the SN-(BN + Al_2O_3) laminates. A strong effect of the layer thickness on the apparent fracture toughness was observed for all thickness up to ~230 μm, followed by a slight decrease in the apparent fracture toughness (Fig. 9). This decrease in the apparent fracture toughness above ~230 μm is not clear at this point. One possible explanation could be the decrease in strength of the interface as its thickness becomes smaller compared to the thickness of the Si_3N_4 layers.

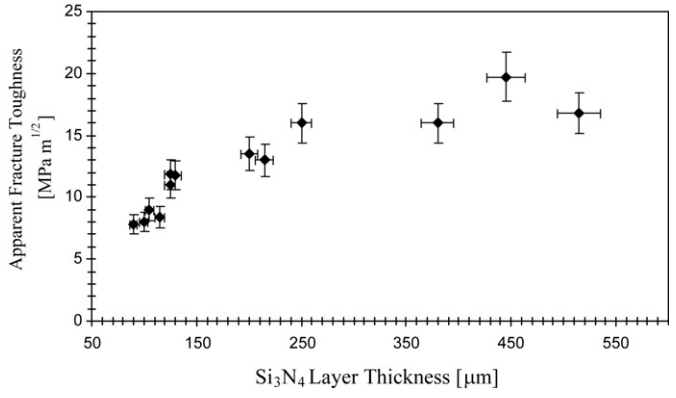

Fig. 8. Effect of Si_3N_4 layers thickness on fracture toughness of SN-(BN + SN) laminated structure.

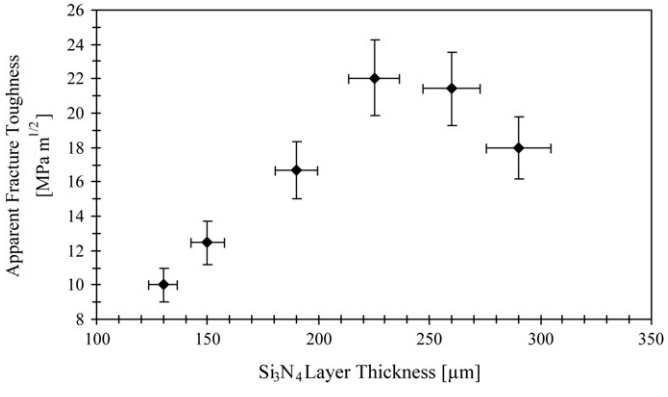

Fig. 9. Apparent fracture toughness vs. Si_3N_4 layer thickness in (BN + Al_2O_3) laminates with 7 layers.

4. Conclusion

Pull out and crack deflection along the weak interface are found to be the dominant mechanisms of toughening of the concentric Si_3N_4/BN laminated structures. The highest apparent fracture toughness of 22 MPa $m^{1/2}$ was found in SN-(BN + Al_2O_3) laminates having 7 Si_3N_4 layers with an average thickness of 230 μm. In the SN-(BN + SN) laminates, the highest apparent fracture toughness of 19.5 MPa $m^{1/2}$ was found with the samples having 4 Si_3N_4 layers with an average thickness of 430 μm. Due to the presence of the weak interfaces and repeated crack initiation across each Si_3N_4 layers, the laminated structures exhibit no notch width sensitivity which, in the past, was found only in fibre composites.

Crack deflection and its reinitiation at the next Si_3N_4 layers are found to be the two dominant factors which control the apparent fracture toughness. High density of the Si_3N_4 layers which resists crack initiation on its surface is favourable condition for a crack deflection at the interface and it is responsible for the high fracture toughness in SN-(BN + Al_2O_3) laminates.

References

1. Clegg, W. J., Kandall, K., Alford, N. M., Birchall, D. and Button, T. W., A simple way to make tough ceramics. *Nature*, 1990, **347**, 455–457.
2. She, J., Inoe, T. and Ueno, K., Multilayer Al_2O_3/SiC Ceramics with improved mechanical behavior. *J. Eur. Ceram. Soc.*, 2000, **20**, 1771–1775.
3. Sanchez-Herencia, A. J., Pascual, C., He, J. and Lange, F. F., ZrO_2/ZrO_2 Layered composites for crack bifurcation. *J. Am. Ceram. Soc.*, 1999, **82**, 1512–1518.
4. Mawdsley, J., Kover, D. and Halloran, J. W., Fracture behavior of alumina/monazite multilayer laminates. *J. Am. Ceram. Soc.*, 2000, **83**, 802–808.
5. Yu, Z., Krstic, Z. and Krstic, V. D., Laminated Si_3N_4/SiC composites with self-sealed structure. *Key Eng. Mater.*, 2005, **280–283**, 1873–1876.
6. Krstic, Z. and Krstic, V. D., Young's Modulus, density and phase composition of pressureless sintered self-sealed Si_3N_4/BN laminated structures. *J. Eur. Ceram. Soc.*, 2008, **28**, 1723–1730.
7. Liu, H. and Hsu, S. M., Fracture behavior of multilayer silicon nitride/boron nitride ceramics. *J. Am. Ceram. Soc.*, 1996, **79**, 2452–2457.
8. Zhang, L. and Krstic, V. D., High toughness silicon carbide/graphite laminar composite by slip casting. *Theor. Appl. Fract. Mech.*, 1995, **24**, 13–19.
9. Clegg, W. J., The fracture and failure of laminar ceramic composites. *Acta Metall. Mater.*, 1992, **40**, 3085–3093.
10. Phillips, A. J., Clegg, W. J. and Clyne, T. W., Fracture behavior of ceramic laminates in bending I: modeling of crack propagation. *Acta Metall. Mater.*, 1993, **41**(3), 805–817.
11. Kübler, J., Fracture toughness of ceramics using the sevnb method: preliminary results. *Ceram. Eng. Sci. Proc.*, 1997, **18**(4), 155–162.
12. Krstic, Z., Yu, Z. and Krstic, V. D., Effect of grain width and aspect ratio on mechanical properties of Si_3N_4 ceramics. *J. Mater. Sci.*, 2007, **42**, 5431–5436.